JOURNAL OF SEMICONDUCTOR TECHNOLOGY AND SCIENCE, VOL. 21, NO. 6, DECEMBER, 2021 ISSN(Print) 1598-1657
https://doi.org/10.5573/JSTS.2021.21.6.418 ISSN(Online) 2233-4866

A New Coupling Spring Design for MEMS Tuning Fork Structures Demonstrating Robustness to Fabrication Errors and Linear Accelerations

Faisal Iqbal[1], Hussamud Din[1], Seungoh Han[2], and Byeungleul Lee[1,*]

Abstract—**This paper presents a new coupling spring design for the MEMS tuning fork structure. The spring design incorporates the outer arm, inner arm, and torsional arm. The outer and inner arms are connected through the torsional arm to be rotationally symmetric, constituting 180° in relation to the center of spring. The designed coupling spring always prioritizes an anti-phase motion providing robustness to linear acceleration. The operation of the spring was validated through FEM simulations and experimental results. The experimental results demonstrated that the anti-phase resonant frequency was 27,280 Hz, whereas the in-phase resonant frequency was 27,780 Hz. Furthermore, the designed coupling spring benefited from a narrow etch cavity and small surface area, making it an ideal design for consumer electronics applications.**

Index Terms—

I. INTRODUCTION

With improved performances, low cost, and compact size, MEMS tuning fork (MEMS-TF) structures are widely used as gyroscopes [1-3] and resonators [4-6]. The MEMS-TF structures consist of two masses and are operated in anti-phase motion. These masses can be either coupled mechanically or electrostatically.

In electrostatically coupled resonators, it is challenging to achieve perfect anti-phase motion since the fabrication errors are inevitable, and it is almost impossible to fabricate two masses with the same frequency [7]. To overcome this issue, mechanically coupled resonators have been proposed [8-10]. One of the issues with mechanically coupled structures are the unwanted in-phase motion, which lies at a frequency lower than the required anti-phase frequency. Also, with the fabrication errors, both of the resonant modes can be merged.

MEMS-TF structures are believed to have the advantage of resisting linear accelerations, when operated in an anti-phase mode. However, structure asymmetry and spring unbalancing caused by the fabrication errors make MEMS-TF vulnerable to linear accelerations. The effect of acceleration sensitivity (g-sensitivity), on the performance of MEMS-TF structures has been presented widely [7, 9, 11-14], so it is essential to reduce the effect of linear accelerations (g-sensitivity) on these structures.

Several design approaches have been reported to improve the g-sensitivity of mechanically coupled MEMS tuning fork structures, Singh [10, 15] studied the effect of linear accelerations, showing that the frequency decoupling ratio between the in-phase and anti-phase modes can improve the acceleration sensitivity. To further improve the resistance to linear accelerations and increase the decoupling ratios, different spring architectures are proposed, such as lever mechanism [16,

Manuscript received Jun. 3, 2021; reviewed Oct. 8, 2021; accepted Oct. 10, 2021
[1]School of Mechatronics Engineering, Korea University of Technology and Education, 31253, Korea
[2]Department of Robotics and Automation Engineering, Hoseo University, 31702, Korea
E-mail : bllee@koreatech.ac.kr

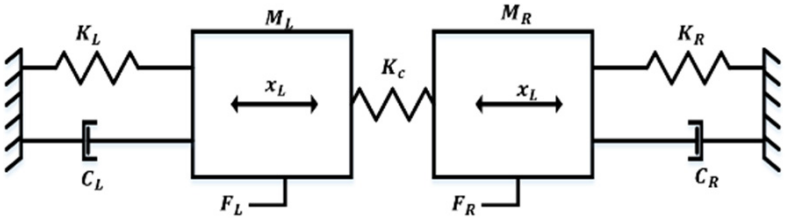

Fig. 1. Two degrees of the model for MEMS tuning fork.

17], z-beam coupling spring [18], diamond-shaped [19], circular-shaped [8, 20], T-shaped [21], lozenge-shaped [22], and polygon-shaped [23]. Most of the proposed spring architectures presented exhibit either large surface area or wide etch cavities. The large size of the spring will increase the device size, making it difficult to use in specific applications such as consumer electronics, whereas the wide etch area will make these springs more prone to fabrication errors.

In this article, a new coupling spring architecture has been proposed to overcome the previous spring designs' issues. The proposed design benefits with the miniaturization and narrow etch cavity, making it more robust to the fabrication errors. The proposed coupling spring always prioritizes the anti-phase motion by keeping the unwanted in-phase motion at a higher frequency, providing robustness to linear accelerations.

II. THE DESIGN CONCEPT OF THE MEMS TUNING FORK RESONATOR

The MEMS tuning fork resonator's conceptual design, which can be modeled as two degrees of freedom system, is shown in Fig. 1. The two identical masses, left mass (M_L), and right mass (M_R), are anchored through the left and right spring, K_L and K_R, respectively. Also, both the masses are mechanically coupled through coupling spring K_c to form a shared resonance. The coupled resonators shown in Fig. 1 can be modeled as a second-order spring-mass system as shown below:

$$M_L\ddot{x}_L + C_L\dot{x}_L + K_L x_L + K_c\left(x_L - x_R\right) = F_L \quad (1)$$

$$M_R\ddot{x}_R + C_R\dot{x}_R + K_R x_R + K_c\left(x_R - x_L\right) = F_R \quad (2)$$

Here, $M, C,$ and K represent the mass, damping, and spring constant of the resonator, and subscripts R and L represent the right and left sides. F_L and F_R are the applied forces. Eqs. (1) and (2) can be solved for the in-phase and anti-phase motions by assuming $M_L = M_R = M$, $C_L = C_R = C$ given by [6, 19]:

$$\ddot{x}_{in} + \frac{\omega_{in}}{Q_{in}}\dot{x}_{in} + \omega_{in}^2 x_{in} = \frac{(F_L + F_R)}{M} + \frac{K_L - K_R}{2M}x_{an} \quad (3)$$

$$\ddot{x}_{an} + \frac{\omega_{an}}{Q_{an}}\dot{x}_{an} + \omega_{an}^2 x_{an} = \frac{(F_L - F_R)}{M} - \frac{K_R - K_L}{2M}x_{in} \quad (4)$$

In this equation, $x_{an} = x_L - x_R$ is the anti-phase motion, $x_{in} = x_L + x_R$ is the in-phase motion, $\omega_{in} = \sqrt{(K_L + K_R)/M}$ and $\omega_{an} = \sqrt{(K_L + K_R + 4K_c)/M}$ represents the in-phase and anti-phase resonant frequencies, and $Q_{an} = M\omega_{an}/c$ and $Q_{in} = M\omega_{in}/c$ are the anti-phase and in-phase quality factors respectively.

From Eqs. (3) and (4), it is clear that the in-phase and anti-phase resonant modes depend on the polarity of the applied force and the coupling spring. The design goal for the coupling spring, as discussed above, is to have an anti-phase resonant frequency lower than the spurious in-phase resonant frequency, occupying a small surface area and narrow etch cavity. This can be achieved by the proposed anti-phase coupling spring architecture shown in the Fig. 2.

The proposed anti-phase spring architecture is comprised of outer, inner, and torsional arms. The outer arms are connected to the masses, M_L and M_R. Meanwhile, one side of the inner arms is anchored, while the other side is connected to the outer arm through the torsional arm in a rotationally symmetric manner, constituting 180° in relation to the center of the coupling spring. The deformation of the designed spring during the lateral load and axial load is shown in the Fig. 2(a) and (c) respectively. During the lateral load the outer

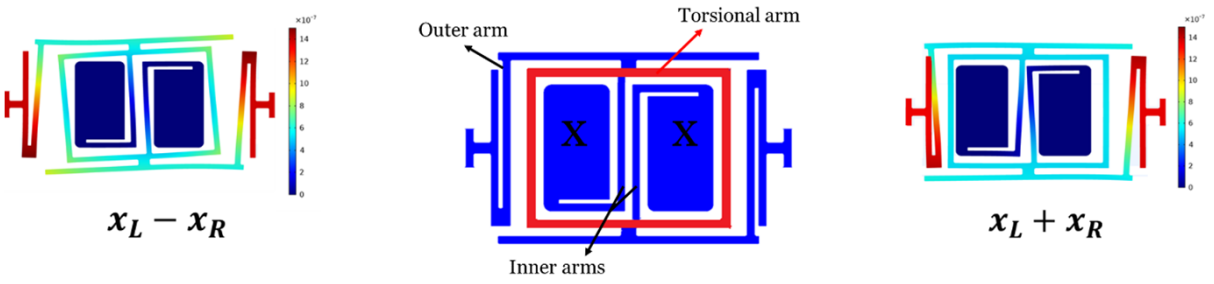

Fig. 2. Proposed coupling spring architecture (a) spring deformation during anti-phase motion, (b) designed spring, (c) spring deformation during in-phase motion.

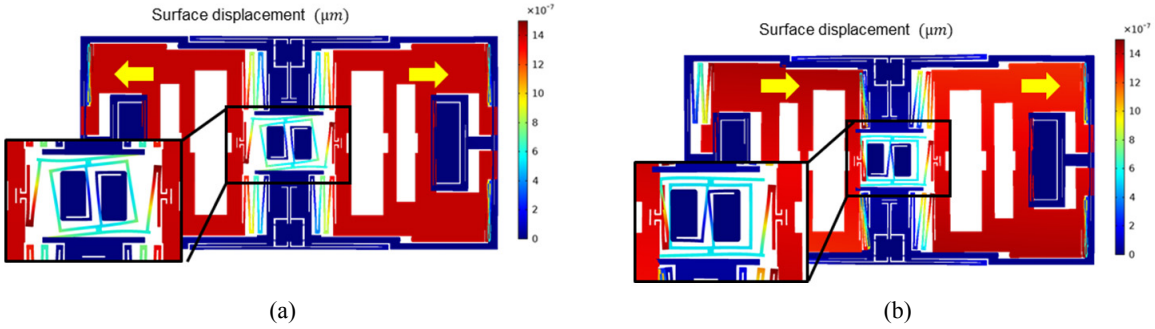

Fig. 3. Resonant mode of the tuning fork resonator (a) anti-phase resonant mode, (b) in-phase resonant mode.

arms move in the opposite direction, whereas the inner arms move in the same direction, in such a way that the torsional arm rotates along the lateral axis. The rotation of the torsional arm lessens the resistance for a low frequency anti-phase resonant mode. However, during the axial load, both the outer arms bend in the same direction, whereas the inner arms bend in the opposite direction. This opposite motion of the inner arm resist the motion of the torsional arm, resulting in a high frequency in-phase resonant mode.

The proposed spring architecture prioritizes the anti-phase motion, providing resistance to linear acceleration and robustness to fabrication imperfections with the narrow cavity holes. Resonant modes of the designed MEMS-TF resonator utilizing the anti-phase coupling spring architecture are shown in the Fig. 3.

III. FEM Simulations

The designed MEMS-TF resonator was investigated through FEM simulation using COMSOL Multiphysics. The resonator was simulated as single-crystal silicon having a Young modulus of 179 *GPa* and poison ratio of 0.29. A triangular mesh with a minimum element size of 0.1 μm was used, consisting of 120 K triangular elements. Frequency domain study was used to investigate (i) the anti-phase operation of the proposed coupling spring and (ii) the effect of linear acceleration on the resonant modes of the MEMS-TF resonator.

3.1 Anti-phase Operation

FEM simulations validated the mechanically forced anti-phase motion. Initially, a balanced force of $0.2\ \mu N$ was applied to both the masses M_R and M_L. The force F_R and F_L are acting on M_R and M_L, respectively, as shown in Fig. 4(a).

The frequency response function along with the phase is shown in Fig. 5(a). It can be observed that both masses are displaced in the anti-phase, having a maximum displacement of $3\ \mu m$ at a resonant frequency of 29,760 *Hz*. This configuration is standard among MEMS-TF resonators to achieve anti-phase motion, also called electrical coupling or indirect coupling.

The MEMS fabrication errors are inevitable, causing

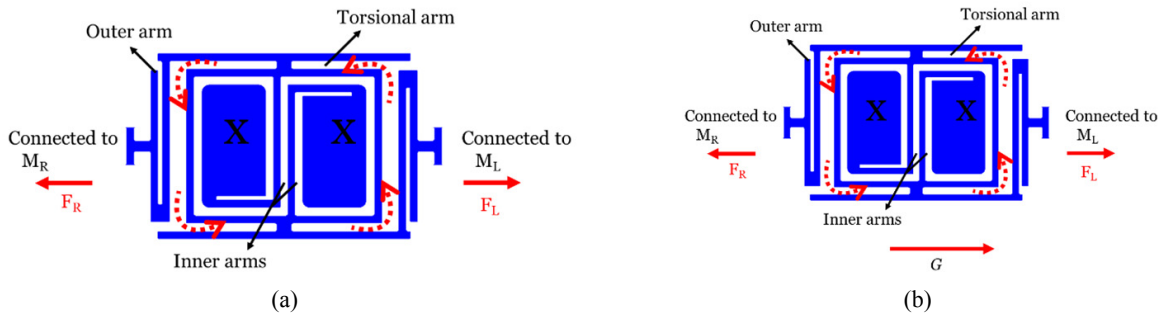

Fig. 4. (a) Anti-phase link mechanism with balance actuation, (b) anti-phase link with balance actuation and under the influence of linear acceleration.

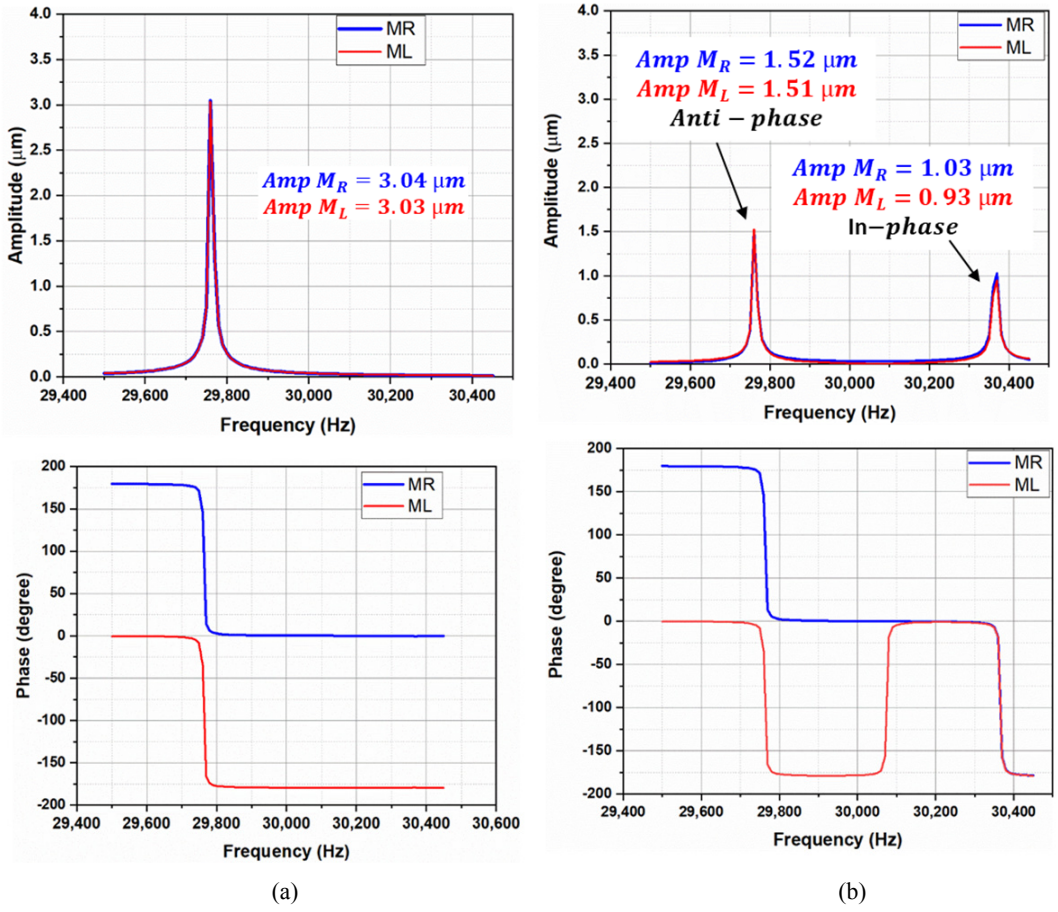

Fig. 5. The frequency response of the tuning fork structure (a) with balance actuation ($FL = -FR$), (b) frequency response of the tuning fork resonator when a single side force is applied.

mass imbalance, spring imbalance or force imbalance to the tuning fork structure. To study the effect of imbalance force and robustness to the fabrication errors, one of the force was set to zero; i.e., $F_R = 0$. This means that a single side force was applied to the MEMS-TF resonator. The frequency response function for this configuration is shown in Fig. 5(b). It can be observed that, the in-phase motion occurred at a higher frequency of 30,370 *Hz*. Here, it is worth mentioning that the anti-phase motion still dominants, having a displacement of $1.5\mu m$.

3.2 Effect of Linear Accelerations

To study the effect of linear acceleration, a balanced

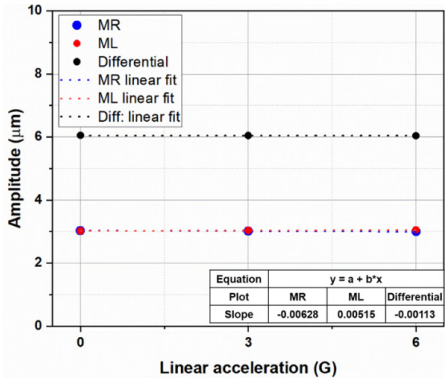

(a)

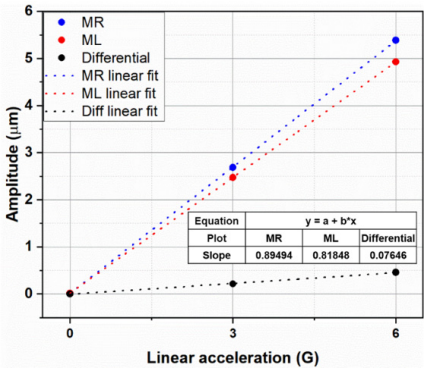

(b)

Fig. 6. (a) Linear sensitivity of the anti-phase mode, (b) linear sensitivity of the in-phase mode.

force of $0.2\,\mu N$ was applied to both masses in opposite directions to actuate the MEMS-TF resonator differentially. Furthermore, a linear force was applied along the x-axis i.e. along the direction of actuation, as shown in Fig. 4(b). The linear force corresponds to a linear acceleration, ranging from $0\,G$ to $6\,G$, where, $1\,G = 9.8\,m/sec^2$.

The effect of linear acceleration on the anti-phase resonant mode is shown in the Fig. 6(a). It can be observed that at $0\,G$ both the masses M_L and M_R had been displaced by $3\,\mu m$ due to the balanced differential force, whereas the overall differential displacement of $6\,\mu m$ was achieved. Furthermore, the displacement of both the independent masses, as well as the overall differential displacement was evaluated under the linear acceleration of $3G$ and $6G$. By linear fitting, it was observed that the linear acceleration sensitivity of the independent masses, M_L and M_R were $-6\,nm/G$ and $5\,nm/G$ respectively, whereas the differential sensitivity was $1.1\,nm/G$.

The same procedure was followed to study the effect of linear acceleration on the in-phase resonant mode, where the results are shown in the Fig. 6(b). It can be observed that at $0\,G$, the net displacement i.e. both of the individual masses as well as differential displacement was zero, due to balance differential force. However, at high G, it was observed that the in-phase mode was more susceptible to the linear accelerations. The individual masses had an acceleration sensitivity of $89\,nm/G$, while the differential output corresponded to $76.4\,nm/G$. This shows that the anti-phase mode is 69.45 times more resilient to the linear acceleration.

IV. Experimental Results

The equivalent electrical model and test method of the fabricated MEMS-TF resonator is shown in Fig. 7(a), while the optical image of the fabricated device using the designed coupling spring is shown in Fig. 7(b). The resonator was fabricated using three wafer stacked processes (i.e., device wafer, via wafer, and cap wafer), with a device thickness of $30\,\mu m$ and vacuum-sealed at $100\,mtorr$.

The resonator was actuated by electrostatic force with an AC voltage of $v_{ac} = 100\,mV_{pk}$ and a DC polarization voltage of $V_{DC} = 5\,V$. The drive circuitry generates the differential signal; i.e., $V_{DP} = V_{DC} + v_{ac}$ and $V_{DN} = V_{DC} - v_{ac}$. The sense current was converted to the sense voltage using a charge amplifier, and the frequency response function (FRF) was computed through the Zurich instrument (MFLI).

4.1 Characterization

4.1.1 Differential Balance Force

The frequency response of the left mass and right mass with balance differential force is depicted in Fig. 8, showing both the masses moving in anti-phase motion (i.e., $180°$ out of phase, with an amplitude response of $40\,mV$ and $39\,mV$). The anti-phase resonant frequency was $27,280\,Hz$. A comparison of simulation

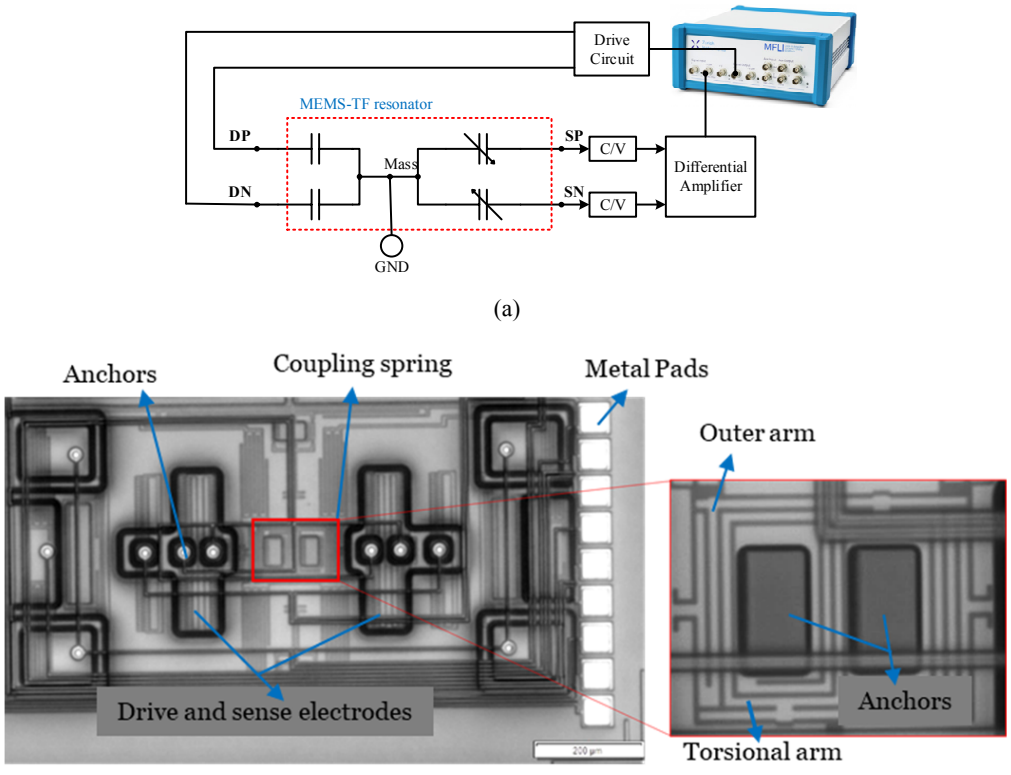

Fig. 7. (a) Electrical modal and experimental setup, (b) optical photograph of wafer-level vacuum packaged MEMS-TF resonator (captured by EMI PHEMOS-1000).

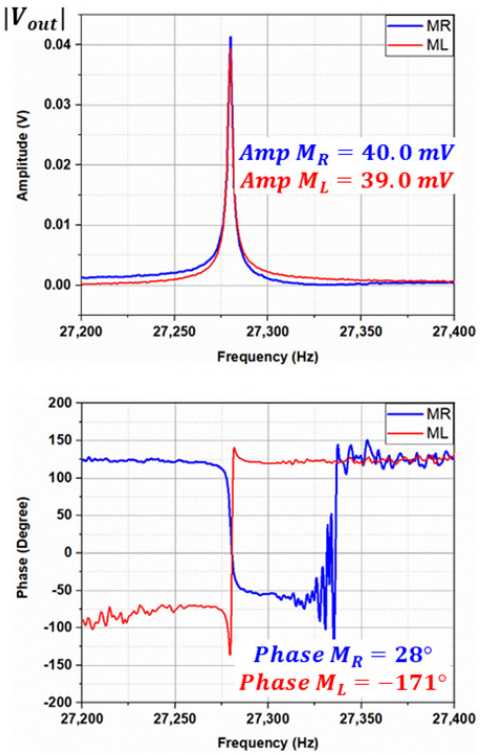

Fig. 8. Anti-phase resonant mode with balance-anti-phase force.

and experimental results depicted a phase error of 19^{o} between the two masses. It was found that the phase error arises from the parasitic feed-through signal, i.e. the drive signal has been coupled to sense signal through parasitic capacitances. The phase error can be minimized by implementing the feed-through cancellation scheme as discussed in [2].

4.1.2 Single Side Force

When actuated by the single side, the resonant masses' frequency response is shown in Fig. 9. During the anti-phase motion, as shown in Fig. 9(a), it can be observed that the output voltage is almost halved of the amplitude, $18\ mV$, compared to the differential actuation, since the force is halved, while the phase error was measured to be $13°$. Meanwhile, the in-phase motion was observed at a higher frequency of $27,780\ Hz$, with an amplitude of $0.4\ mV$, as shown in Fig. 9(b). It is worth mentioning that, with the single side force, the in-phase mode is suppressed by $97.7\ \%$, while the coupling spring prioritizes the anti-phase motion.

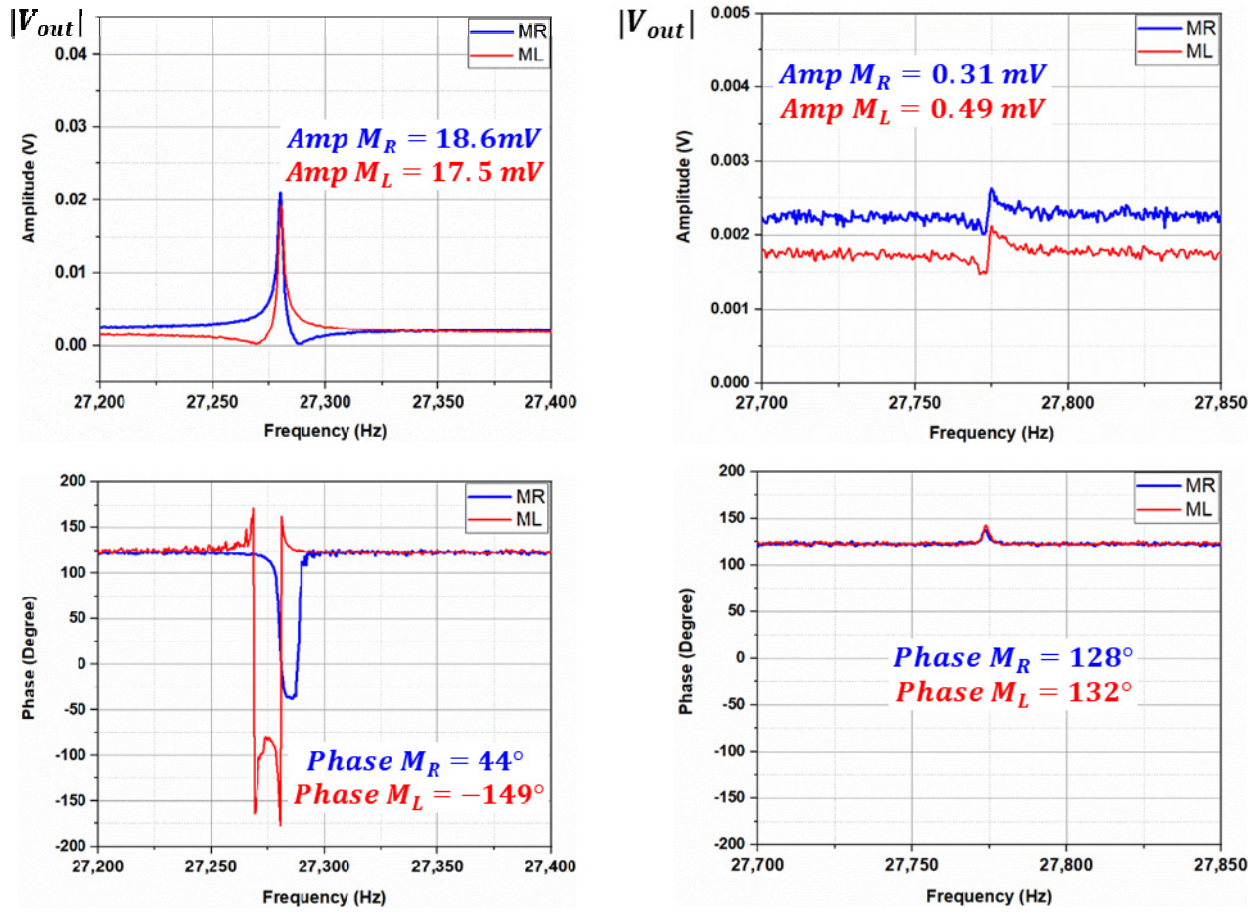

(a) (b)

Fig. 9. Frequency response of the MEMS-TF resonator with single side force (a) anti-phase response, (b) in-phase response.

V. CONCLUSION

This study has successfully demonstrated a new coupling spring design for MEMS tuning fork structures. The new coupling spring design provides perfect anti-phase motion at a lower resonant mode while keeping the surplus in-phase resonant mode high. The designed coupling spring has low etched cavities, making it more robust to fabrication errors and small surface area, resulting in a wide range of device applications. The FEM simulations were carried out to study the effect of linear accelerations and un-balanced forces. The in-phase mode is more susceptible to the linear accelerations, showing that the individual masses have an acceleration sensitivity of $89\ nm/G$, whereas the differential output corresponds to $76.4\ nm/G$. This shows that the anti-phase mode is 69.45 times more resilient to the linear acceleration. Furthermore, experimentally, the designed coupling spring architecture suppresses the in-phase mode by 97 %.

Author Contributions: Conceptualization, Faisal Iqbal, Seungoh Han and Byeungleul Lee; Formal analysis, Faisal Iqbal; Software, Faisal Iqbal and Hussamud Din; Experiment, Faisal Iqbal; Supervision, Byeungleul Lee; Writing—original draft, Faisal Iqbal; Writing—review and editing, Faisal Iqbal, Hussamud Din, and Byeungleul Lee.

ACKNOWLEDGEMENT

This work is supported by the R&D program of the Ministry of Trade, Industry, and Energy (MOTIE)/Korea Evaluation Institute of Industrial Technology (KEIT). (10084665, Development of IMU Embedded 6-axis, 10-axis compound navigation system integrating highly reliable inertial measurement unit (IMU), Global

Navigation Satellite System (GNSS), Magnetometer, and altimeter for maned/unmanned aircraft).

This work was (partially) supported by the post-doc scholarship program of KOREATECH.

REFERENCES

[1] F. Iqbal, H. Din, and B. Lee, "Single Drive Multi-Axis Gyroscope with High Dynamic Range, High Linearity and Wide Bandwidth," *Micromachines,* vol. 10, p. 410, 2019.

[2] F. Iqbal, M. A. Shah, and B. Lee, "Analysis of parasitic feed-through capacitance in MEMS gyroscope with push pull configuration," in *2017 IEEE 12th International Conference on Nano/Micro Engineered and Molecular Systems (NEMS)*, 2017, pp. 414-417.

[3] A. Walther, C. Le Blanc, N. Delorme, Y. Deimerly, R. Anciant, and J. Willemin, "Bias contributions in a MEMS tuning fork gyroscope," *Journal of microelectromechanical systems,* vol. 22, pp. 303-308, 2012.

[4] F. Iqbal and B. Lee, "A Study on Measurement Variations in Resonant Characteristics of Electrostatically Actuated MEMS Resonators," *Micromachines,* vol. 9, p. 173, 2018.

[5] T.-A. W. Roessig, "Integrated MEMS tuning fork oscillators for sensor applications," 1999.

[6] S. A. Zotov, B. R. Simon, I. P. Prikhodko, A. A. Trusov, and A. M. Shkel, "Quality factor maximization through dynamic balancing of tuning fork resonator," *IEEE Sensors Journal,* vol. 14, pp. 2706-2714, 2014.

[7] P. Janioud, A. Koumela, C. Poulain, P. Rey, A. Berthelot, P. Morfouli*, et al.*, "Tuning the Anti-Phase Mode Sensitivity to Vibrations of a MEMS Gyroscope," in *Multidisciplinary Digital Publishing Institute Proceedings*, 2017, p. 355.

[8] K. Azgin, Y. Temiz, and T. Akin, "An SOI-MEMS tuning fork gyroscope with linearly coupled drive mechanism," in *2007 IEEE 20th International Conference on Micro Electro Mechanical Systems (MEMS)*, 2007, pp. 607-610.

[9] Y. Gao, H. Li, L. Huang, and H. Sun, "A lever coupling mechanism in dual-mass micro-gyroscopes for improving the shock resistance along the driving direction," *Sensors,* vol. 17, p. 995, 2017.

[10] P. S. Thakur, K. Sugano, T. Tsuchiya, and O. Tabata, "Experimental verification of frequency decoupling effect on acceleration sensitivity in tuning fork gyroscopes using in-plane coupled resonators," *Microsystem technologies,* vol. 20, pp. 403-411, 2014.

[11] S. W. Yoon, S. Lee, and K. Najafi, "Vibration-induced errors in MEMS tuning fork gyroscopes," *Sensors and Actuators A: Physical,* vol. 180, pp. 32-44, 2012.

[12] A. Koumela, C. Poulain, C. Le Goc, T. Verdot, L. Joet, P. Rey*, et al.*, "Resilience to vibration of a tuning fork MEMS gyroscope," *Procedia Engineering,* vol. 168, pp. 1725-1730, 2016.

[13] Y. Guan, S. Gao, H. Liu, and S. Niu, "Acceleration sensitivity of tuning fork gyroscopes: Theoretical model, simulation and experimental verification," *Microsystem Technologies,* vol. 21, pp. 1313-1323, 2015.

[14] F. Giacci, S. Dellea, and G. Langfelder, "Signal integrity in capacitive and piezoresistive single-and multi-axis MEMS gyroscopes under vibrations," *Microelectronics Reliability,* vol. 75, pp. 59-68, 2017.

[15] T. P. Singh, K. Sugano, T. Tsuchiya, and O. Tabata, "Frequency response of in-plane coupled resonators for investigating the acceleration sensitivity of MEMS tuning fork gyroscopes," *Microsystem technologies,* vol. 18, pp. 797-803, 2012.

[16] A. Trusov, A. Schofield, and A. Shkel, "Gyroscope architecture with structurally forced anti-phase drive-mode and linearly coupled anti-phase sense-mode," in *TRANSDUCERS 2009-2009 International Solid-State Sensors, Actuators and Microsystems Conference*, 2009, pp. 660-663.

[17] A. A. Trusov, A. R. Schofield, and A. M. Shkel, "Micromachined rate gyroscope architecture with ultra-high quality factor and improved mode ordering," *Sensors and Actuators A: Physical,* vol. 165, pp. 26-34, 2011.

[18] H. Din, F. Iqbal, and B. Lee, "Modelling and optimization of single drive 3-axis MEMS gyroscope," *Microsystem Technologies,* pp. 1-9, 2020.

[19] Y. Guan, S. Gao, H. Liu, L. Jin, and S. Niu, "Design and vibration sensitivity analysis of a

MEMS tuning fork gyroscope with an anchored diamond coupling mechanism," *Sensors,* vol. 16, p. 468, 2016.

[20] Y. Guan, S. Gao, L. Jin, and L. Cao, "Design and vibration sensitivity of a MEMS tuning fork gyroscope with anchored coupling mechanism," *Microsystem Technologies,* vol. 22, pp. 247-254, 2016.

[21] A. Sharma, F. M. Zaman, B. V. Amini, and F. Ayazi, "A high-Q in-plane SOI tuning fork gyroscope," in *SENSORS, 2004 IEEE*, 2004, pp. 467-470.

[22] T. Q. Trinh, L. Q. Nguyen, D. V. Dao, H. M. Chu, and H. N. Vu, "Design and analysis of a z-axis tuning fork gyroscope with guided-mechanical coupling," *Microsystem technologies,* vol. 20, pp. 281-289, 2014.

[23] Q. Xu, Z. Hou, Y. Kuang, T. Miao, F. Ou, M. Zhuo, *et al.*, "A tuning fork gyroscope with a polygon-shaped vibration beam," *Micromachines,* vol. 10, p. 813, 2019

Faisal Iqbal received his B.S. degree in Telecommunication Engineering from University of Engineering and Technology, Peshawar, Pakistan. He received his MS and Ph.D. degree in Interdisciplinary Program in Creative Engineering from Korea University of Technology and Education, Republic of Korea, in 2017 and 2020, respectively. He is currently working as a Research Fellow at Queen's University Belfast, United Kingdom. Previously, he worked as Postdoctoral researcher at Korea University of Technology and Education for 1 year. His research interests include MEMS based inertial sensors.

Hussamud din received his B.S. degree in Electronics Engineering from International Islamic University, Islamabad, Pakistan in 2011, and M.S. degree in Electrical Engineering from Center for Advanced Studies in Engineering, Islamabad, Pakistan in 2016. He is currently pursuing his Ph.D. degree in Mechatronics Engineering at Korea University of Technology and Education, Cheonan, South Korea. His research interests include MEMS inertial sensors and energy harvesters.

Seungoh Han received his B.S., M.S., and Ph.D. degrees in electrical engineering at Korea University (Seoul, Korea) in 1996, 1998, and 2006, respectively. Since 2007, he has been working for Hoseo University (Asan, Korea) as a professor. His current research interests include smart sensors, MEMS/NEMS, and coupled-physics analysis of micro/nano-devices.

Byeungleul Lee is Professor at Korea University of Technology and Education. He received his B.S. degree in Electronics Engineering from the Hanyang University, and M.S. degree in Electrical and Electronics engineering from Korea Advanced Institute of Technology in 1989 and 1991, respectively. He obtained his Ph.D. in Electrical Engineering and Computer Science from the Seoul National University in 2004. From 1991 to 2008, he worked for Samsung Electronics as a principal researcher for MEMS development. His research interests include semiconductor transducer and MEMS applications.